COMPUTER SIMULATION OF [010](010) DISLOCATIONS IN ANTHRACENE CRYSTALS

NAOKI IDE*, I. OKADA and K. KOJIMA
Graduate School of Integrated Science* and Department of Physics, Yokohama City University, 22-2 Seto, Kanazawa-ku, Yokohama 236, Japan

ABSTRACT

The equilibrium configurations for the cores of [010](001) edge and screw dislocations in an anthracene crystal were calculated using the atom-atom potential method. A boundary condition has been examined in which molecular rotations were taken into account together with translational displacements on the basis of anisotropic elasticity. The edge dislocation had a spread-out shear misfit and the width of Burgers vector density at half peak height reached 6.2 times the magnitude of the Burgers vector. The molecular configurations for the screw dislocation was strongly anisotropic and its core region did not spread. The energy of the screw dislocation was lower than that of the edge dislocation. The Peierls stresses of both the edge and screw dislocations were estimated by means of increasing gradually an external stress. That of the screw dislocation was much larger than that of the edge dislocation.

INTRODUCTION

In organic crystals, the role of structural defects is important not only in diffusion and mechanical properties, but also in many other phenomena such as solid-state reactions, photoplastic effects, and the formation of local electronic states of polarization origin and exciton trapping states of structural origin [1,2]. To make clear how defects are concerned with these phenomena, investigations into the microscopic structure of the defects are essential. Computer simulation is used to reveal the details of the local structure around the defects. In the case of crystal of aromatic hydrocarbons, such as anthracene, consisting of nonpolar molecules, weak intermolecular forces of the Van der Waals force are essential and the atom-atom potential methods have been used.

The equilibrium configuration for the core of a dislocation in a crystal of aromatic hydrocarbons was first calculated by Mokichev and Pakhomov [3] for a [010](001) edge dislocation in naphthalene crystals. The model used consisted of the inner layer of 72 mobile molecules and the outer fixed layer on the basis of isotropic elasticity. The Peierls stress in organic crystals was first obtained for polyethylene in an orthorhombic phase using computer simulation by Bacon and Tharmalingam [4]. However, for aromatic hydrocarbons, such as anthracene, any calculation of the Peierls stress has not been reported yet.

In anthracene crystals, a (001)[010] slip system and a (001)[110] system are dominantly operative [5,6,7]. In present paper, we will report the molecular configurations around a [010](001) edge dislocation [8] and a screw dislocation, and their Peierls stresses [9]. One problem of particular interest was what structure of the dislocation core is realized in the crystal composed of disk-like molecules possessing rigid body. Orientational aspects characteristic of molecular crystals were studied in detail. We introduced molecular rotations into initial and boundary conditions to a linear approximation, as well as translational displace-

ments in terms of anisotropic elasticity, because the dimensions of an anthracene molecule are as large as the magnitude of the Burgers vector. The Peierls stresses were estimated by means of increasing an external stress step by step until the dislocation moved over a length of an unit lattice vector.

The molecule was assumed rigid and the atom-atom potential method was used. Both the methods of static energy minimization and of molecular dynamics were used to obtain equilibrium configurations. A model of size sufficient to study the molecular configurations in crystals composed of the large molecule was adopted with the aid of a supercomputer.

POTENTIAL AND METHOD

A perfect crystal of anthracene with monoclinic symmetry (space group $P2_1/a$) has two nonequivalent molecules, one at the corner of a basal unit lattice (hereafter referred to as a corner molecule), and the other at the center (a center molecule). There are a glide symmetry between these two kinds of molecules and a twofold screw symmetry.

We begin by constructing the regular lattice, which is stable under a given potential. The functional form used for the atom-atom potential is the Buckingham function

$$\phi_{ij}(r_{ij}) = -A_{ij}/{r_{ij}}^6 + B_{ij}\exp(-C_{ij}r_{ij})$$

where r_{ij} is the distance between non-bonded atoms and A, B and C are empirical parameters presented by Williams [10] in set IV [11,12,13]. The cut-off radius of interaction between atoms was 8 Å throughout this paper. The evaluated lattice constants using this potential were $a_0 = 8.18$ Å, $b_0 = 5.91$ Å, $c_0 = 11.17$ Å, $\beta = 2.16$, $\theta = 1.17$, $\phi = 1.11$ and $\psi = 1.91$, and the packing energy per molecule was 1.02 eV.

Our model for dealing with the relaxation of molecules around the dislocation consists of two layers. One is the outer rigid layer where molecules are held in the positions described later. The other is the inner layer, which consists of the relaxable molecules whose centers lie within the cylinder of radius $r_{\rm rel}$ with its center at the dislocation line. An anisotropic linear elasticity of the dislocation is used in those layer. Translational displacements u in terms of anisotropic elasticity can be derived from the general equation given by Hirth and Lothe [14]. The elastic constants used there are obtained by constituting strained lattices and differentiating their energies numerically by the strains.

In addition to translational displacements, we introduce molecular rotations into the initial and boundary conditions to a linear approximation, because the dimensions of an anthracene molecule are as large as the magnitude of Burgers vector. Molecular rotations proportional to strains are estimated from displacements and the changes in Euler angles per unit strains. Deformations, in general, are accompanied by rigid body rotations ($\frac{1}{2}\mathrm{rot}u$) and these also cause molecules to rotate. The magnitudes of these rotations are estimated at the center of molecules, and these two kinds of molecular rotations are added. To simulate an infinitely-long, straight dislocation, periodic boundary conditions are imposed along the dislocation line.

To obtain the equilibrium configuration of molecules in the inner layer, we have tried both the methods of static energy minimization and molecular dynamics. In the static minimization, a method of steepest descent is applied repeatedly until all matrices $(\partial^2 E_{\rm MR}/\partial x_i \partial x_j)$ become positive definite and remain so for about ten steps (where $E_{\rm MR}$ denotes the energy of a molecular row parallel to the dislocation line). Then a Newton method is used to make convergence rapid. In the molecular dynamics, the crystal is quenched ev-

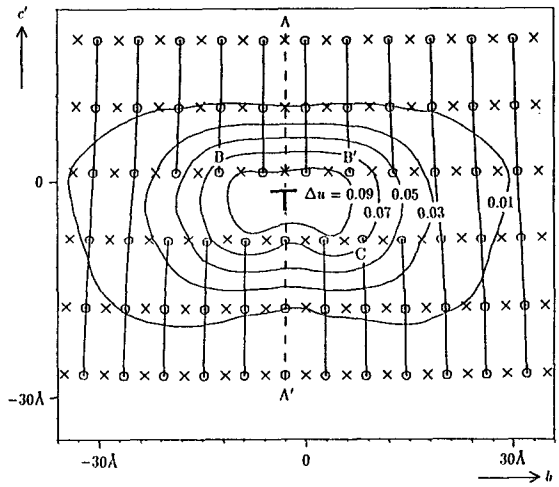

Figure 1. Projection in the bc' plane of molecular centers after relaxation and equipotential curves Δu (in eV). Crosses denote the corner molecules and circles denote the center molecules.

ery time the total kinetic energy reaches a maximum [15]. It was confirmed that the two methods gave the same result as regards the molecular configurations.

To evaluate the effects of the model size on molecular configurations, several runs were made using $r_{\rm rel}$=4b (24 Å) $\sim$ 16b (96 Å). It was confirmed that $r_{\rm rel}$ = 16b was sufficient to obtain the equilibrium configuration. Results of calculations, which will be shown later, were obtained by the use of this size.

THE EDGE DISLOCATION

The center of the dislocation for the initial and boundary conditions was put at the point where the energy after relaxation were minimum. The coordinate of that point was $(y,\ z) = (\frac{1}{4}b_0,\ \frac{7}{8}c'_0)$, where c'_0 is a unit length of the c' axis. The upper limit of convergence error was estimated to be 4 meV/a_0 for the largest model with $r_{\rm rel}$ = 16b (96 Å, 1062 molecules in the inner layer).

Equilibrium configurations around the edge dislocation

Figure 1 shows a projection in the bc' plane of molecular centers after relaxation and equipotential curves Δu around the dislocation; Δu is the packing energy per unit lattice relative to that of a perfect crystal. It is obvious that the dislocation has a spread-out shear misfit along the slip plane, and that a rectangular region where the energies Δu are almost equal exists around the center of the dislocation. The plane AA′ through the center of the dislocation is almost a symmetry plane. Equipotential curves became smooth only if the energies of a corner molecule and a center molecule were summed, because effects of the shear strain ε_{23} on two kinds of molecules are different; for example, energies of molecules just below the slip plane are 30 meV ($l_2 = -\frac{3}{2}$, where l_2 denotes the lattice site along x_2 direction), 45 (-1), 39 ($-\frac{1}{2}$), 47 (0), 33 ($\frac{1}{2}$), 33 (1), 51 ($\frac{3}{2}$), 39 (2), 40 ($\frac{5}{2}$), 27 (3). The equipotential curves are slightly asymmetric in the core region, as pointed out in a naphthalene crystal by Mokichev and Pakhomov [3]. The high energy region spreads widely, in comparison to the

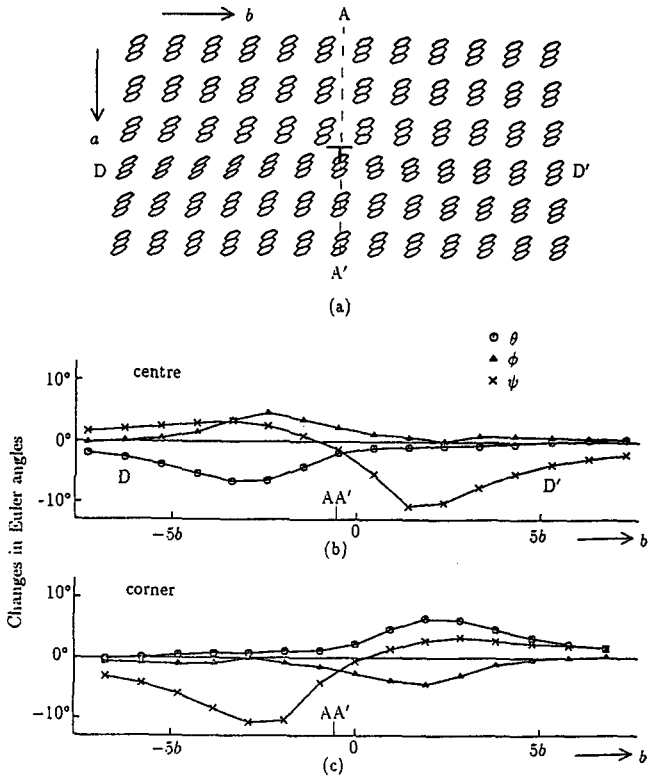

Figure 2.
Orientational aspects of molecules around the dislocation: (a) projection in the *ab* plane of center molecules, (b) changes in Euler angles of the center molecules in the *ab* plane just below the slip plane, and (c) those of the corner molecules.

result in a naphthalene crystal.

The distribution of strain ε_{22} in the direction parallel to the slip plane was also calculated. The value of the strain is small even in the core region since the core spreads wide. Its maximum value is only 7% in the upper half plane and its minimum value is −5% in the lower half plane.

Orientational aspects of molecules around the dislocation were investigated in detail. It is shown in figure 2(a) that the changes in the Euler angles are larger on the side with the extra half planes than on the other. The changes in the Euler angles of the center molecules in the plane just below the slip plane are shown in figure 2(b), and those of the corner molecules are shown in figure (c). It is obvious from these diagrams that the changes reach maxima not at the center but at the distance $2b \sim 3b$ from the center of the dislocation; $\Delta\theta = 6.5°$, $\Delta\phi = 4.6°$, $\Delta\psi = 10.7°$. Curves in (a) and (b) indicate that there is some approximate symmetry between the corner and the center molecules with respect to the plane AA′. That symmetry is glide-symmetry-like; this may come from the fact that there is the glide symmetry between the two kinds of molecules in the perfect crystal and the shear stress around the dislocation is antisymmetric with respect to the plane AA′. It would be a true glide symmetry if two kinds of molecules were distributed continuously in each plane.

Distribution densities of the Burgers vector

Figure 3 shows distribution densities of the Burgers vector along the basal slip plane, ρ_y

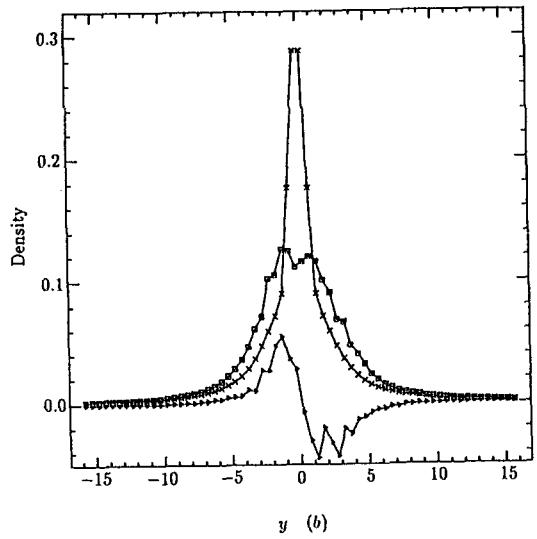

Figure 3. Distribution densities of the Burgers vector along the basal slip plane, ρ_y and ρ_x. Crosses: ρ_y before the relaxation; squares: ρ_y after the relaxation; triangles: ρ_x after the relaxation.

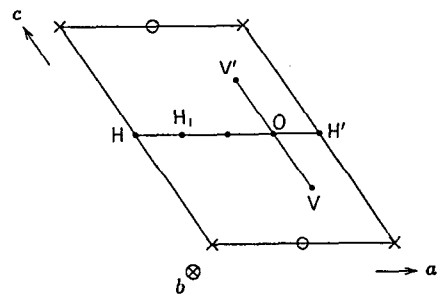

Figure 4. A projection in the ac plane of a perfect crystal. Crosses denote the corner molecules and circles denote the center molecules. The influence on the dislocation energy of changing the position of the dislocation for the boundary condition was evaluated on the lines HH′ and VV′.

and ρ_x [16]. The density after relaxation deviates substantially from that before relaxation in a wide range from the center to about $8b$. The core of the dislocation was not dissociated into two typical partials, but was spread widely. The width of the core at half peak height is large, being $6.2b$ for the relaxed crystal, in comparison with $2b$ for the unrelaxed crystal. It is seen from the ρ_x in the figure that only the molecules close to the center of the dislocation deviate from the molecular plane, and that this deviation is small.

THE SCREW DISLOCATION

Figure 4 shows a projection in the ac plane of a unit cell of a perfect crystal. The perfect crystal of anthracene has a twofold screw axis parallel to the b axis at the point O. The coordinate of the point O is $\frac{3}{4}a_0 + \frac{1}{2}c_0$, where a_0 and c_0 are unit lattice vectors. The dislocation line is set to run along the b axis.

To search for an adequate position of the dislocation for the initial and boundary conditions, the center of the dislocation was put at various points along the lines HH′ and VV′ in the figure. The energies after relaxation were compared for these cases using the relaxation radius $r_{\mathrm{rel}} = 6b$. Among the dislocations with centers on the line HH′, that with its center at the point O has the lowest energy and that with its center at the point H_1 has the

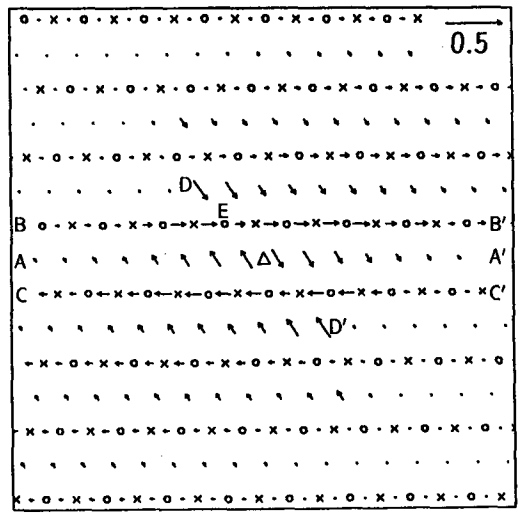

Figure 5. A projection in the ac plane of molecular centers around a [010](001) screw dislocation. Δ denotes the center of dislocation; o the center molecule; × the corner molecule. The length of arrows indicates the magnitude of the strain $\varepsilon_{2\theta}$. The molecule to which an arrow point is more displaced along x_2 direction than the other molecule connected by the arrow.

highest energy. Inequality between O and H_1 comes from the fact that the direction of the corner molecule is different from that of the center molecules. Among dislocations centered on the line VV′, that with its center at the point O has the lowest energy. Consequently the center of the dislocation will be set at the point O in the following simulations.

Equilibrium configurations around the screw dislocation

Figure 5 shows a projection in the ac plane of molecular centers and the distribution of a shear strain $\varepsilon_{2\theta}$ ($1/r\ \partial u_2/\partial\theta$, where θ is an angle from the x_1 axis) after the relaxation. the distribution of the strain $\varepsilon_{2\theta}$ is strongly anisotropic even in a elastic solution. It is due to anisotropy of elastic constants.

A elastic constant $c'_{2\theta 2\theta}$ in terms of the cylindrical coordinates (r, θ, x_2) has a minimum value, 1.46 GPa in the direction of $\theta = 40.3°$, and a maximum value, 4.78 GPa in the direction of $\theta = -49.7°$. Since the latter is 3 times larger than the former, the distribution of the strain $\varepsilon_{2\theta}$ is strongly anisotropic. The direction for the smallest elastic constant is approximately normal to molecular planes and rotations of molecules are easy when a shear stress is applied in that direction.

The distribution of a shear strain $\varepsilon_{2\theta}$ is not influenced by the relaxation on the slip plane AA′. Rotations of molecules around normal axes of molecules contribute to the strain on that plane, so that the strain can concentrate near the dislocation center to the same extent as in the elastic solution. The maximum value of the strain reaches 20%, while that of a compressive strain was only 5% around the edge dislocation. The distribution spreads out a little on the planes BB′ and CC′, on which molecules lie closely and the strain is prevented from concentrating in a narrow region. Shear strains at the point D and D′ are large, but actual displacements are slight due to the fact that the angles subtended by the dislocation center are small. Figure 6 shows distribution densities of the Burgers vector along the basal slip plane, $\rho_y(x)$. The density after relaxation deviates only a little from that before relaxation.

The molecular configuration, concerning positions and orientations, has a complete

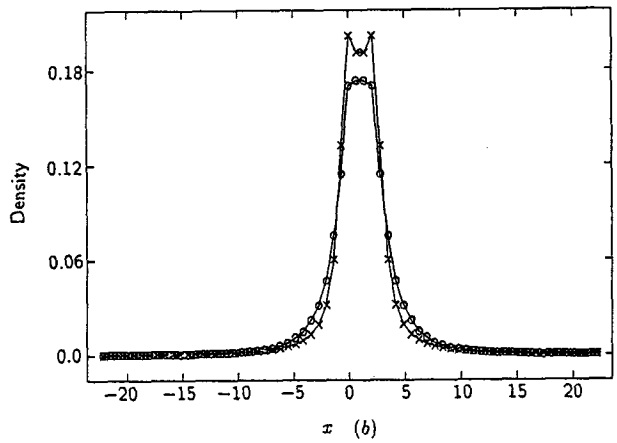

Figure 6. Distribution densities of the Burgers vector along the basal slip plane, $\rho_y(x)$; crosses denote before the relaxation, circles after that.

twofold symmetry with respect to the dislocation center, while that of a perfect crystal has a twofold screw symmetry. The changes in Euler angle reach maxima near the center; $\Delta\theta = 6.3°$, $\Delta\phi = 1.2°$ and $\Delta\psi = 14.5°$. The changes in $\Delta\psi$ are large and this indicates that rotations around the normal axes of molecular planes are main ones in the core of the screw dislocation.

Energy distribution

The energy distribution spreads a little along the slip plane near the center, and in the region far from the center, though the energy is low, it spreads in the direction of $\theta = 40°$ from a axis. A high energy region does not, however, spread so much as that of the edge dislocation. The maximum value of the strain energy at the dislocation center is 0.02 eV smaller than that of the edge dislocation, although the shear strain of the screw dislocation is large at the center.

The strain energy W per repeated distance b_0 of an screw dislocation may be written as

$$W = E_d \ln(R/r_0)$$

where E_d is called the prelogarithmic energy factor, r_0 is called the effective core radius and R is the outer radius of a circular cylinder within which the energy is evaluated. The value of E_d was estimated to be 0.27 eV/b_0 from the anisotropic elastic constants for the screw dislocation, 0.60 eV/a_0 for the edge dislocation.

A prelogarithmic energy factor of the screw dislocation after the relaxation is 0.27 eV/b_0, which agrees very well with that from the elasticity, and is smaller than that of the edge dislocation, 0.57 eV/a_0. An energy within the cylindrical region of radius $5b_0$ is 0.64 eV/b_0, which is smaller than that of the edge dislocation, 1.28 eV/a_0. These show clearly that the energy of the screw dislocation is lower than that of the edge dislocation. The effective core radius r_0 was estimated to be $0.45b_0$ for the screw dislocation, and $0.53b_0$ for the edge dislocation.

PEIERLS STRESS

Method

The model of crystal is the same as that used for the determination of the structure of dislocation. The Peierls stress can be obtained using the following iterative procedures. The stable molecular configuration around the dislocation under no external stress (i.e. $\sigma_{ex} = 0$), such as obtained in the previous section, is taken as the initial state.

The external stress is increased by $\Delta\sigma_{ex}$ at the beginning of each step. In the present calculation, the increment $\Delta\sigma_{ex}$ has only one component ε_{23}. We take 2×10^{-4} and 1×10^{-2} μ as the value of the increment for the edge and the screw dislocation, respectively, where μ is the shear modulus; $\mu = (c_{44}c_{66} - c_{46}^2)^{1/2} = 2.65$ GPa. All the molecules in the crystal are translated in proportion to the strain caused by the external stress. In addition to this translation of molecules, the molecular rotation corresponding to the strain is taken into account to a linear approximation, as described above.

Then the relaxations are repeated until any component of the displacement vectors of relaxable molecules during one relaxation process becomes less than certain criterion [17]. As the value of the criterion, we adopted 1×10^{-5} (in Å or rad), because the same results were obtained for the criterion smaller than this. We employed only the Newton method with line search as the relaxation method.

After the relaxation, the position of the dislocation is examined; the position along the slip plane is defined as

$$y_d = \frac{\int y\rho_y(y)dy}{\int \rho_y(y)dy} \qquad \text{and} \qquad x_d = \frac{\int x\rho_y(x)dx}{\int \rho_y(x)dx}$$

for the edge and the screw dislocation, respectively. If the position of the dislocation moves more than one lattice repeat distance from its initial position, the external stress at that step is regarded as the Peierls stress.

Results

In the case of the edge dislocation, the value of the Peierls stress decreased largely as relaxation radius increased, but it saturated for the model larger than $r_{rel} = 8b$. The extrapolated value of the Peierls stress to infinitely large model, τ_P(edge), was $0.8 \sim 1.0 \times 10^{-3}$ μ. In the case of the screw, the value of the Peierls stress was quite little affected by the choice of the model size. The extrapolated value to infinitely large model, τ_P(screw), was $1.9 \sim 2.0 \times 10^{-1}$ μ. From comparison between the Peierls stress of the edge and that of the screw, it is surmised that the plastic deformation in the present slip system of anthracene crystals would be controlled by the screw dislocations at low temperature.

DISCUSSION

It was found that the edge dislocation in an anthracene crystal had the spread-out shear misfit along the slip plane. The distribution density ρ_y of the Burgers vector along the

slip plane deviated largely from that of the elastic solution in the wide range from the center to a distance $8b$. This seems to be a characteristic feature of aromatic crystals, because strains could not converge into a narrow region due to the large rigid bodies of molecules. This dislocation had some symmetry, which looked like a glide symmetry.

The distribution of the shear strain $\varepsilon_{z\theta}$ around the screw dislocation was strongly anisotropic and the molecular configurations had a complete twofold symmetry with respect to the dislocation center. Its core region did not spread unlike that of edge dislocation. The shear strain that was a main strain in the screw dislocation could become large near the dislocation center, since rotations of molecules around the normal axes of molecules were easy and contributed to this strain. The energy of the screw dislocation was, however, lower than that of the edge dislocation.

It was found from the present simulation that the value of the Peierls stress of the screw dislocation was much larger than that of the edge dislocation. This is consistent with the relation of the core widths of the dislocations, i.e., that the core width of screw is narrower than that of the edge. The anthracene crystals is brittle below about 100 K, and fractures by the external stress without plastic deformations. The extrapolation of yield stress to 0 K using the experimental values at the temperature from 110 to 150 K gives $4.6 \times 10^{-3}\ \mu$ [7]. This value is between the calculated Peierls stress of the edge and that of the screw, but the latter is considerably high.

To investigate the causes for the high Peierls stress of the screw, we tried to elucidate the shape of the Peierls potential. The dislocation whose center is put on arbitrary position in a unit lattice as an initial condition moves to the position such that the whole energy is minimized by the relaxation. The whole energy after the relaxation would be expressed as

$$E(x_\mathrm{f},\ x_\mathrm{i}) = E_\mathrm{P}(x_\mathrm{f}) + E_\mathrm{inc}(x_\mathrm{i},\ x_\mathrm{f}),$$

where x_i and x_f indicate the positions of the dislocation along the slip plane before and after the relaxation, respectively. The first term on the right side, $E_\mathrm{P}(x_\mathrm{f})$, represents the Peierls potential, and becomes minimum at $x_\mathrm{f} = x_0$, where x_0 corresponds to the point O in figure 4. The second term, $E_\mathrm{inc}(x_\mathrm{i},\ x_\mathrm{f})$, denotes the elastic energy caused by the inconsistency of the position of the moved dislocation with that in the outer fixed region. We supposed this energy to be expressed as

$$E_\mathrm{inc}(x_\mathrm{i},\ x_\mathrm{f}) = \frac{1}{2}k(x_\mathrm{f} - x_\mathrm{i})^2,$$

where k is constant. The dislocation is in equilibrium after the relaxation so that $d/dx_\mathrm{f}\ E_\mathrm{P}(x_\mathrm{f}) = -k(x_\mathrm{f} - x_\mathrm{i})$. The relation between $x_\mathrm{f} - x_0$ and $x_\mathrm{f} - x_\mathrm{i}$ can be actually obtained from the computer simulation, as shown in figure 7(a). This relation is obviously linear so that we may put $x_\mathrm{f} - x_\mathrm{i} = -g(x_\mathrm{f} - x_0)$, where g is constant. The estimation of the gradient g gives 3.46. Using this relation, the functional form of the Peierls potential is determined as

$$E_\mathrm{P}(x_\mathrm{f}) = \frac{1}{2}gk(x_\mathrm{f} - x_0)^2$$

and the whole energy E is rewritten as

$$E(x_\mathrm{f}) = \frac{1}{2}C(x_\mathrm{f} - x_0)^2,$$

where $C = gk(1+g)$. The coefficient C can be obtained from the simulation, as shown in figure 7(b). The estimation of the value of C gives 4.85×10^{-1} eV/$a_0{}^2 b_0$ so that k=25.5 MPa. Thus, we obtain the Peierls potential between $x_\mathrm{f} = \frac{3}{4} - 0.114$ and $x_\mathrm{f} = \frac{3}{4} + 0.114$ (in a_0), which are referred to as A and B, respectively, below. In the vicinity of the minimum of the

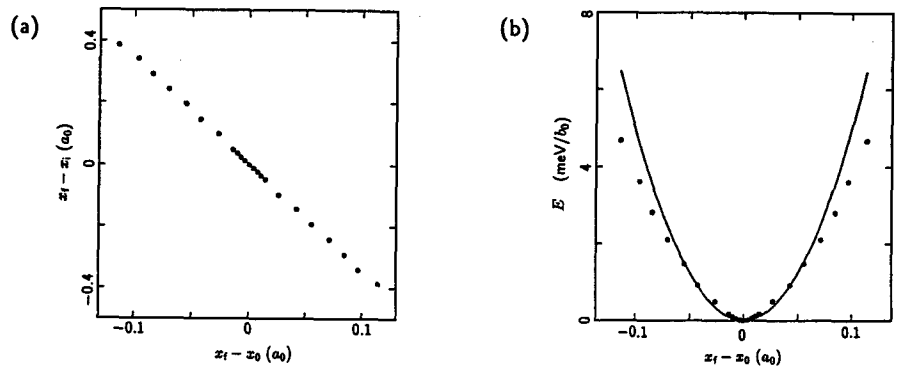

Figure 7. The relation between $x_f - x_i$ and $x_f - x_0$ (a) and the that between E and $x_f - x_0$ (b). These relations were obtained using the model size $r_{rel} = 6b$.

Peierls potential, A–B, the potential curve is smoothly parabolic and there is no section at which the gradient is so steep that the Peierls stress becomes very large.

By the relaxation under the condition that the twofold symmetry with respect to the dislocation center is conserved, the screw dislocation centered on the position H_1 in figure 4, which corresponded to the saddle point in the energy space, can be relaxed remaining its center fixed at the position ($x_f = x_i = \frac{1}{4}a_0$); its energy is 2.23×10^{-2} eV/b_0. There would exist the section with the large gradient causing the high Peierls stress in the range in which the Peierls potential cannot be estimated.

To confirm that the high Peierls stress is caused not by an undesirable behavior in numerical treatments (such as falling into a local minimum), but by the characteristic features in anthracene crystals, we also tried to perform the molecular dynamics, in which the potential barrier between a local and the absolute minimum can be overridden owing to the kinetic energy. The model crystal is the same as that used in static method, and only the molecules in the inner region can move under the condition that the temperature and the strain applied to the outer fixed region is kept constant. The periodic boundary condition used above is applied also in this case. It should be noted that this calculation using molecular dynamics is performed not to reproduce actual phenomena, but to confirm the result obtained at 0 K.

Figure 8 shows the time developments of the center of the dislocation under the stress $\sigma_{ex} = 10^{-1}\ \mu$ at the temperature of 15, 20, 25 and 35 K. The screw dislocation can move above 25 K, but does not move within 35 pico second below 20 K. Making the several similar runs using the different values of the external stress, we obtained the relation between the temperature and the external stress which could move the dislocation within 35 ps, as shown in figure 9. This figure means that the macroscopic plastic deformation takes place easily on the right of the curve, and is hard to take place on the left of that. Even under a half stress of τ_P(screw), the dislocation must override the barrier corresponding to 20 K. This diagram shows that the calculated Peierls stress is not too high in comparison with the external stress at low temperature. Hence, it may be sure that the screw dislocation has the high Peierls stress within our model. It was also found from this figure that the mobility of the screw dislocation has the strong dependence on temperature. This would suggest the possibility that the yield stress of anthracene crystals also depends strongly on the temperature at low temperature.

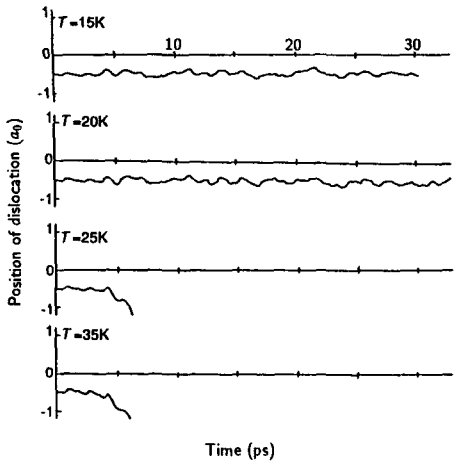

Figure 8. The time developments of the center of the dislocation under the stress $\sigma_{ex} = 10^{-1}\ \mu$ at 15, 20, 25 and 35 K.

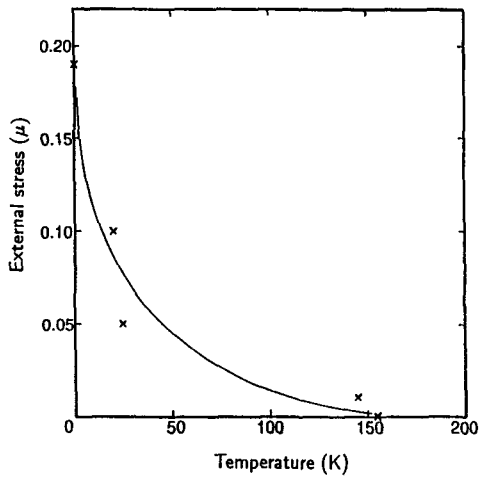

Figure 9. The dependence on temperature of the external stress required to move the dislocation within 35 ps. The stress at 0 K is the Peierls stress.

Figure 10. The forces acting on the molecule E and its neighbors projected onto ab plane. Arrows show the vectors of the force acting on an atom. The molecule E is show in figure 5.

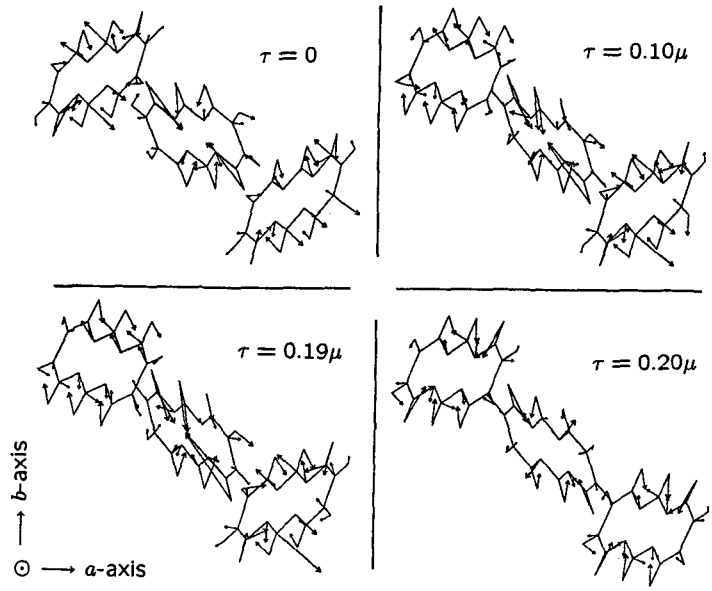

The molecule marked E in figure 5 suffers the quite large forces from the surrounding molecules, as shown in figure 10. This would mean that the molecular configuration around the molecule E is very stable to the external shear stress σ_{23} so that the strain caused by this stress, particularly ε_{12}, cannot be increased in this region; ε_{12} is significant to the movement of the screw dislocation. This seems to result in the high Peierls stress.

The Peierls stress obtained through the present model may be lowered if something which can change the molecular configuration around E, such as the deformation of molecules, the effect of the stress component except σ_{23} and so on, is taken into account. Even if the

value of the Peierls stress of the screw dislocation were lowered, however, from comparison between the core width of screw dislocation and that of edge, it would be certain that the plastic deformation in present slip system is controlled by the screw dislocations at low temperature.

ACKNOWLEDGEMENTS

We would like to thank the staff of the Computer center of Yokohama City University for useful advice. The numerical calculations were partially carried out at the Computer center of Tokyo University. This work was supported in part by a Grant-in-Aid for Scientific Research from the Ministry of Education, Science and Culture, Japan and also by a Grant-in-Aid from Yokohama City.

REFERENCES

[1] E. A. Silinsh, *Organic Molecular Crystals* (Berlin, Springer, 1980), p. 139
[2] A. J. Pertsin and A. I. Kitaigorodsky, *The Atom-Atom Potential method* (Berlin, Springer, 1987), p. 338
[3] N. N. Mokichev and L. G. Pakhomov, Sov. Phys. Solid State **24** 1925 (1982)
[4] D. J. Bacon and K. Tharmalingam, J. Mater. Sci. **18** 884 (1983)
[5] P. M. Robinson and H. G. Scott, Acta. Metall. **15** 1581 (1967)
[6] K. Kojima, Phys. Status Solidi A **51** 71 (1979)
[7] K. Kojima and I. Okada, Philos. Mag. A **61** 607 (1989)
[8] N. Ide, I. Okada and K. Kojima, J. Phys.: Condens. Matter **2** 5489 (1990)
[9] N. Ide, I. Okada and K. Kojima, to be published
[10] D. E. Williams, J. Chem. Phys. **45** 3770 (1966)
[11] D. P. Craig and B. R. Markey, Chem. Phys. Lett. **62** 223 (1979)
[12] A. Dautant and L. Bonpunt, Mol. Cryst. Liq. Cryst. **137** 221 (1986)
[13] I. Okada, M. Sugawara and K. Kojima, J. Phys.: Condens. Matter **1** 3555 (1989)
[14] J. P. Hirth and J. Lothe, *Theory of Dislocations* (New York, McGraw Hill, 1982), p. 423
[15] J. B. Gibson, A. N. Goland, M. Milgram and G. H. Vineyard, Phys. Rev. **120** 1229 (1960)
[16] V. Viteck, L. Lejcek, and D. K. Bowen, *Interatomic Potential and Simulation of Lattice Defects* (New York, Prenum, 1971) ed. P. Gehlen *et al.*
[17] F. Minami, E. Kuramoto and S. Takeuchi, Phys. Status Solidi A **22** 81 (1974)